

STRONTIUM ZINC FERRITE BY USING HYDROTHERMAL TECHNIQUE

¹AMUTHA@SANTHI.V, ²SANGEETHA.S

^{1,2}Assistant Professor

^{1,2}Department of chemistry

Mailam Engineering College, Mailam

¹v.shanthi1010@gmail.com, ²sangee.sarangapani@gmail.com

ABSTRACT:

Conceptual Sr-Zn ferrite nanoparticles of compound equation $Sr_xZn(1-x)Fe_2O_4$ ($x=0.5, 0.7, 0.9$) are combined by utilizing aqueous procedure at a temperature of $700^{\circ}C$ for 3 hours and pound for a fine powder. The basic investigation through X-ray beam diffraction (XRD) shows the development of spinel cubic structure with a normal glasslike size in the scope of 8.6nm to 13.6nm. The d-dividing and grid boundary increments by expanding the doping grouping of Strontium (Sr). The expansion in cross section boundary and the decline in molecule size with the increment in Strontium substance might be connected to an expected rearranging of Fe^{3+} and Zn^{2+} particles inside octahedral and tetrahedral destinations. The morphology and the porosity is decide by Scanning Electron Microscopy (SEM). A diminishing pattern in the particles size has likewise been watched, which affirms that the precious stone development is being impeded because of the presence of Strontium.

Keywords: Strontium zinc ferrites, hydrothermal technique, structural study, micro-structural study

I. INTRODUCTION

Ferrite nano-precious stones are rich with physical properties; their flexible qualities have made them extremely fascinating material. Zinc ferrite ($ZnFe_2O_4$) is generally concentrated among nanoparticles. The overall recipe of spinel ferrites (XFe_2O_4 ; where X is divalent cation, for example, Zn_{2+} , Ni_{2+} , Co_{2+} , and so forth.) have been reviewed for their overall attractive and electrical properties. For ordinary spinel ferrites, every single trivalent cation possess octahedral destinations where as tetrahedral locales involved by divalent cations. Spinel stage has attractive property which is a lot of touchy to the classification of cations and their portion in the interstitial locales (octahedral and tetrahedral) of spinel cross sections [1].

At the point when Zinc ferrite is in the mass structure, at that point it shows the ordinary spinel structure in which zinc particles are situated at tetrahedral locales, while iron are situated at octahedral destinations [2-3]. This material is helpful at business level and is broadly utilized in a few fields, for example, gas sensors, attractive applications, data stockpiling, impetuses, electronic gadgets and so forth [4, 5]. The Zinc ferrites have properties, which are exceptionally delicate to the dissemination of cations, incorporate conditions and different replacements of progress metals. Various procedures have been utilized to integrate zinc ferrites nanostructures [6, 7]. In any case, the aqueous strategy is one of the best manufactured courses to orchestrate nano-particles from typical to high temperature. At significant level of temperature few nano-particles are precarious, while few are produced with the loss of little amount of materials at raised fume pressure [8].

In this procedure, Strontium doped Zinc ferrite nano-gems are combined by utilizing aqueous technique for basic and smaller scale basic investigation of the composites. The stage investigation and precious stone size is described through X-ray beam diffraction (XRD) and Scanning Electron Microscopy (SEM) is utilized to decide the morphologies. Strontium Zinc ferrite composite is of imperative significance because of its unmistakable attributes and Zn ferrite is a result of its current use in different fields alongside splendid future possibility.

II. MATERIALS AND METHOD

Trial system requires exact weighing of the considerable number of nitrates (strontium, zinc and iron) included into 100ml of refined water though, sodium hydroxide was included into 100ml of refined water in a different measuring utensil. To get a homogeneous arrangement, attractive blending was done at $90^{\circ}C$ by placing

attractive stirrer in the two measuring utensils while put on hot attractive plates. NaOH was included drop by drop into the arrangement of nitrates to get hastens and left the blends for 10 minutes to settle down. Microwaves were then applied for 5 minutes at 254GHz and blend was moved into the flagon and set into the autoclaved machine for 45 minutes and afterward left for 12 hours to be settled with PH esteem saw as 12.7. The blend was centrifuged for 5 minutes at 2500rpm at that point set into the heater at 150°C until dried totally. From that point, the examples were pounded to fine powder and heater to 700°C for 3 hours for additional auxiliary and miniaturized scale basic examination.

III. RESULTS AND DISCUSSION

The powder X-ray beam diffraction examples of blended $Sr_xZn(1-x)Fe_2O_4$ tests for $x=0.5, 0.7, 0.9$ were estimated with a X-beam diffractometer (XRD) with $Cu\ \alpha$ radiation, inside 2θ territory from 10^0 to 70^0 . The surface morphology of the incorporated examples was dissected with the assistance of Scanning Electron Microscopy (SEM).

A. Structural Analysis

The X-ray beam diffraction examples of $Sr_xZn(1-x)Fe_2O_4$ for the structure of $x=0.5, 0.7$ and 0.9 are appeared in Fig.1.

Fig.1 X-ray beam diffraction (XRD)

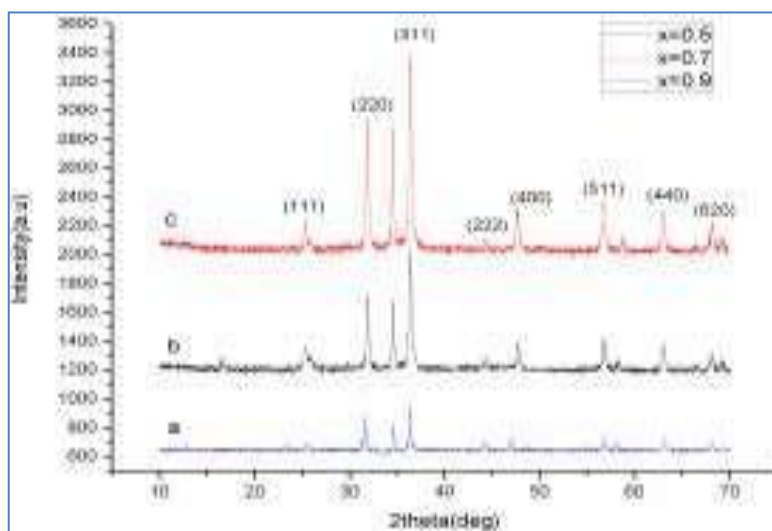
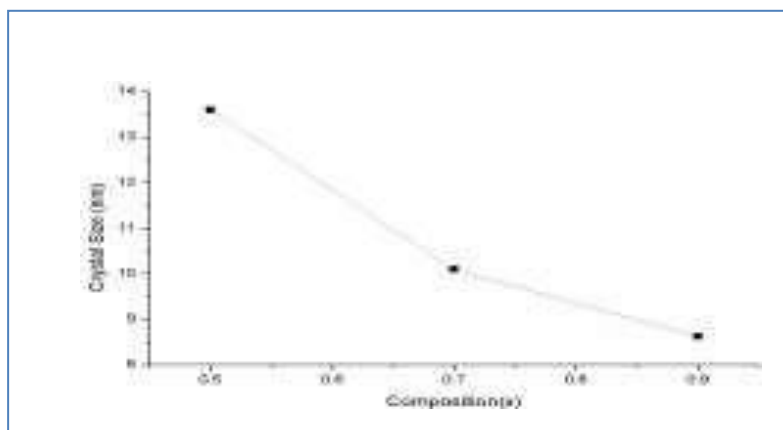


Fig.2 Crystal size fluctuates with arrangement

X-ray beam diffraction (XRD) was done to decide the glasslike structure and stage immaculateness of the materials, blended by utilizing Microwave Hydrothermal strategy. The Sharp and refined pinnacles show that the materials are fundamentally translucent with spinel cubic structure. The nearness of significant cross section planes, for example, (111), (220), (311), (222), (400), (511), (440) and (620) in the given XRD design demonstrate that the dissemination of the precious stones alongside the spinel cubic structure has Fd-3m space bunch [9]. The pinnacles are listed with JCPDs Cards No.82-1049 and 22-1012.

The most unmistakable pinnacles of the examples move to the lower estimations of theta because of the divergence in the range of Sr²⁺(1.44 Å) and Zn²⁺(0.83Å) particles, which offers ascend to little cross section steady and d (between organizer separation) increment the grid strain, appeared in the Table 1. By expanding the convergence of strontium, the precious stone size of the materials diminishes as appeared in Fig.2 and is determined with the assistance of Debye-Scherrer equation [10].

$$D = k\lambda / (\beta \cos\theta) \dots (i)$$

From the given information of plane (311) the molecule size of the example with Sr doping changes between 8.6nm to 13.6nm [11]. Such an exact and diminished size of particles is acquired by shifting the controlling boundaries, including variety of time by applying microwaves from 5 minutes to 10 minutes, temperature and afterward fine crushing.

Table.1 Peak list of Sr_xZn_{1-x}Fe₂O₄ for 311 plane						
Sampl es (X)	2θ (degree)	Intensi ty (a.u)	Crystal Size (nm)	d- spaci ng (Å⁰)	Lattice Parameter a (Å⁰)	Lattice Strain (ε)
X=0.5	36.37	990.33	13.6	2.469919	8.191796	0.0085
X=0.7	36.33	1626.4	10.1	2.472142	8.199170	0.0114
X=0.9	36.31	341.67	8.62	2.473479	8.203603	0.0135

Table.1 Peak List

To ascertain the cross section boundary, utilize the accompanying equation;

$$a = d\sqrt{h^2+k^2+l^2} \dots (ii)$$

Where, "a" is the cross section boundary, "d" is distance between planar dividing/separation and "h k l" are the Miller records. The worth of 'd' is determined by Bragg's law. Grid boundary "a" relies upon the centralization of Strontium.

An expanding pattern with the expansion in convergence of Strontium in the blended nano ferrites is appeared in Fig.3. The expansion in the estimation of grid boundary with the increment in Sr substance can be identified with the distinction of ionic radii of Strontium (1.44 Å) and Zinc (0.83Å) [12, 13]. It plainly shows that as the centralization of Sr builds the cross section boundary "a" would likewise increments, and this occurs due the substitution of Zinc (Zn²⁺) with Strontium (Sr²⁺) [12]. The estimation of grid boundary likewise differs by changing the sintered time. The expanding example of cross section boundary fluctuates directly with the Sr content shows that it additionally complies with Vegard's law estimate [14].

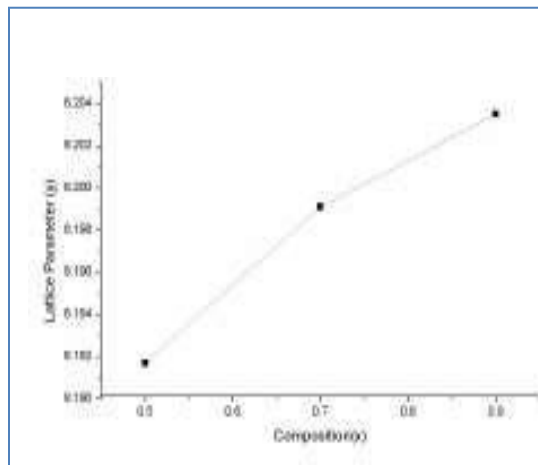


Fig. 3 Lattice boundary Vs composition

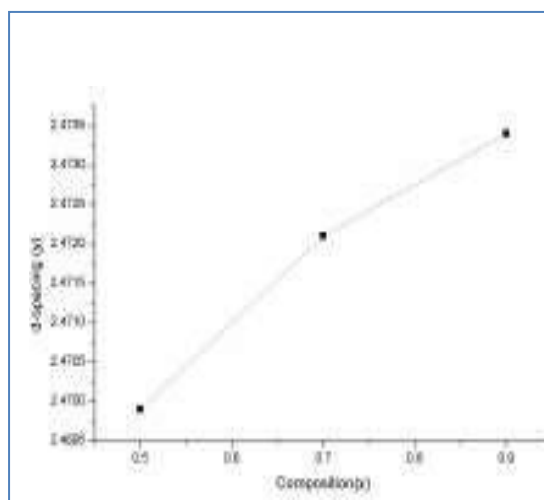


Fig.4 d-spacing Vs composition

The given chart demonstrates the expansion in d-spacing with the expansion in Strontium fixation. The expanding pattern in d-spacing is having a place with the cross section strain which is delivered by the Strontium particles and determined by utilizing the recipe $\epsilon=1/d^2$. With the expansion in Strontium particles the grid strain will likewise increment. It has been demonstrated from the XRD results that the blended nano-ferrites of Strontium doped Zinc Ferrites have a blended spinel structure, which shows that the octahedral destinations would have been obliged by Sr^{2+} and Fe^{3+} and the tetrahedral locales by Zn^{2+} .

B. Scanning Electron Microscopy (SEM) examines

With the estimations of checking electron magnifying lens the surface morphology of the incorporated nano-particles has been distinguished. SEM pictures of the readied Strontium Zinc ferrites nanoparticles are appeared in Fig.5 (a, b, c). The given pictures show that the nanoparticles are consummately orchestrated.

Because of arrival of enormous number of vaporous items, for example, nitrogen, voids and pores are available in the readied tests. The readied nanoparticles are non-uniform and agglomerated; this shape is ascribed to the limitation of grain development [15].

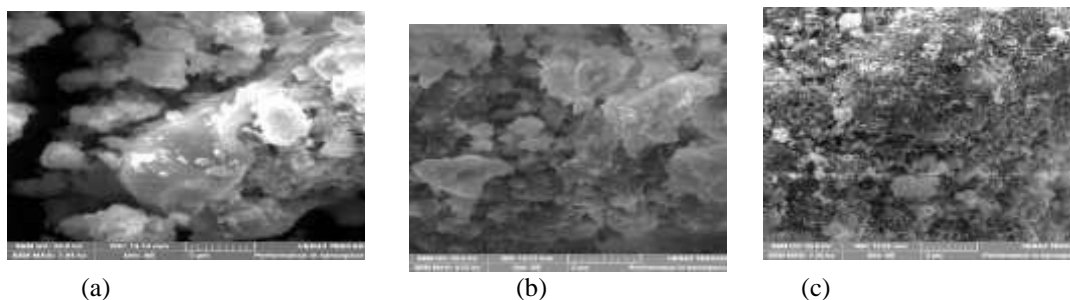


Fig.5 SEM Micrograph for $x= 0.5, 0.7, 0.9$

Fig. 5(a, b, c), gives the data for the arrangement of $x=0.5, 0.7$ and 0.9 at $5\mu\text{m}$. From pictures we can see that the particles are non-uniform and the molecule size is diminished by expanding the amount of strontium from $x = 0.5$ to $x= 0.9$ individually, implies by expanding the strontium the size of precious stone reductions [11, 15]. It obviously shows that the grouping of zinc diminishes by expanding the centralization of strontium, because of which it deters the development of precious stones [16]. The SEM results are effectively fulfilled the XRD examination.

IV. CONCLUSION

Aqueous strategy was utilized to incorporate, $\text{Sr}_x\text{Zn}_{(1-x)}\text{Fe}_2\text{O}_4$ ($x= 0.5, 0.7, 0.9$) for the auxiliary and microstructural contemplates. X-ray beam diffraction completed to break down the precious stone structure, indicated the spinel structure with great crystallinity and stage immaculateness, affirmed by Rietveld investigation. The d-dividing, cross section boundary, mill operator lists and the gem size of the incorporated examples were determined. By expanding the doping grouping of strontium prompted the expansion in d-dividing and in the grid boundary.

REFERENCES

- [1] Zheng, M., Wu, X.C., Zou, B.S., et al., "Magnetic properties of nano-size MnFe_2O_4 particles", *JMMM*, 183, pp. 152–156, 1998.
- [2] Uzma, G., Micro structural and Micro hardness Study of Ni Zn ferrite using Si additive, *J. Sci. Res.*, 5(30), pp. 415-420, 2013.
- [3] Chinnasamy, C.N., Narayanasamy, A., Ponpandian, N., et al., "Magnetic Properties of Nano-structured Ferrimagnetic Zinc Ferrite", *Journal of Physics Condensed Matter*, 12(35) pp.7795–7805, 2000.
- [4] Ehrhardt, H., Campbell, S.J., Hofmann, M., "Magnetism of the nanostructured spinel zinc ferrite", *Scripta Materialia*, 48, pp. 1141-1146, 2003.
- [5] S. Bharadwaj, and S.R.Murthy, "Microwave Hydrothermally Synthesized Nanocrystalline Co-Zn Ferrites", *Integrated Ferroelectrics*, 120(1), pp. 6-14, 2010.
- [6] Ghorbani, H.R.; Mehr, F.P.; Pazoki, H.; et al., "Synthesis of ZnO nanoparticles by precipitation method", *Oriental Journal of Chemistry*, 31, pp. 1219-1221, 2015.
- [7] Yadoji, P., Peelamedu, R., Agrawal, D, et al., "Microwave sintering of Ni-Zn ferrites: Comparison with conventional sintering", *Mater Sci and Engn. B*, 98(3), pp.269–278, 2003.
- [8] A Xia, C Zuo, L Chen, et al. "Hexagonal $\text{rFe}_{12}\text{O}_{19}$ ferrites: hydrothermal synthesis and their sintering properties", *JMMM*, 332, pp. 186-191, 2013.
- [9] Xie, Taiping., Longjun, Xu., Liu, Chenglun., "Dielectric and magnetic response of Sr–Zn ferrite composite", *RSC Advances*, 3(36), pp.15856, 2001.
- [10] Y. Köseoğlu, F. Alan, M. Tan, et al., "Low temperature hydrothermal synthesis and characterization of Mn doped cobalt ferrite nano- particles", *Ceramics International*, 38(5), pp.3625-3634, 2012.
- [11] K. Jalaiah, K.Vijaya Babu, K. "Rajashekhar Babu, and K. Chandra Mouli, Structural and dielectric studies of Zr and Co co-substituted $\text{Ni}_{0.5}\text{Zn}_{0.5}\text{Fe}_2\text{O}_4$ using sol-gel auto combustion method", *Results*

- in Physics*, 9, pp.1417-1424, 2018.
- [12] Gundega Heidemane, Māris kodols, et al. “The Synthesis, Characterization and Sintering of Nickel and Cobalt Ferrite Nanopowders”, *Materials Science (MEDŽIAGOTYRA)* 18(1). 2012.
- [13] Uzma, G., Sadiqua, A., Hayat, Q., A, “Comparative Study on Impact of Nickel Nitrates and Nickel Chloride on the Structural Properties of ZnFe₂O₄ Nanostructures”, *Journal of Nanomaterials & Molecular Nanotechnology*, 7(6)2018, doi: [10.4172/2324-8777.1000256](https://doi.org/10.4172/2324-8777.1000256).
- [14] Azam, A., “Microwave assisted synthesis and characterization of Co doped Cu ferrite nano-particles”, *Journal of Alloys and Compounds*, 540, pp. 145–153, 2012.
- [15] P. S. Hedaoo, D. S. Badwaik, S. M. Suryawanshi, and K. G. Rewatkar, “Structural and Magnetic Studies of Zn Doped Nickel Nanoferrites Synthesize by Sol-gel Auto Combustion Method”, *Materials Today: Proceedings*, 15(3), pp. 416-423, 2019.
- [16] Auwal, I.A, Gungunes, H., Guner, S., et al. Structural, magneto-optical properties and cation distribution of SrBi_xLa_xY_xFe_{12-3x}O₁₉ (0.0 ≤ x ≤ 0.33) hexa-ferrites, *Materials Research Bulletin*, 80, pp.263-272, 2016.